DALTON
FULL PAPER

The synthesis, crystallographic and magnetic characterization of di- and tri-nuclear Ni(II) and Co(II) complexes of (2-sulfanylphenyl)bis(pyrazolyl)methane

Timothy C. Higgs,[a] David Ji,[b] Roman S. Czernuszewicz,[b] K. Spartalian,[d] Charles J. O'Connor,[c] Candace Seip[c] and Carl J. Carrano*[a]

[a] *Department of Chemistry, Southwest Texas State University, San Marcos, TX 78666, USA*
[b] *Department of Chemistry, University of Houston, Houston, TX 77204, USA*
[c] *Department of Chemistry, University of New Orleans, New Orleans, LA 70148, USA*
[d] *Department of Physics, University of Vermont, Burlington, VT 05405, USA*

Received 21st October 1998, Accepted 13th January 1999

The synthesis of a trinuclear thiolate bridged Ni^{II} system, $[Ni_3(L5S)_4]^{2+}$ [L5SH = (2-sulfanylphenyl)bis(pyrazolyl)-methane] which contains a linear NiS_2NiS_2Ni moiety, is reported. Two octahedrally coordinated $(L5S)_2Ni$ complexes, in which the thiol sulfurs are mutually *cis*, constitute the two terminal positions while the central position contains a distorted tetrahedral, four-coordinate, Ni(II) ion. In the presence of alkyl- or aryl-nitriles, such as MeCN, the $[Ni_3(L5S)_4]^{2+}$ cation undergoes cleavage and rearrangement reactions to give thiolate bridged dinuclear dications, either $[Ni_2(L5S)_2(MeCN)_4]^{2+}$ or $[Ni_2(L5S)_2(MeCN)_2(H_2O)_2]^{2+}$, in which MeCN ligand N-donors (and/or H_2O O-donors) occupy the vacant coordination sites of each Ni^{2+} atom. An analogous Co(II) dimer is also reported. The trimer ⟶ dimer reaction can be reversed by desolvation of $[Ni_2(L5S)_2(MeCN)_4]^{2+}$ or $[Ni_2(L5S)_2(MeCN)_2(H_2O)_2]^{2+}$ by an appropriate non-nitrile solvent, such as $MeNO_2$ resulting in reformation of the $[Ni_3(L5S)_4]^{2+}$ cation. Variable temperature magnetic data indicate that the Ni atoms in the trimer are weakly antiferromagnetically coupled while they are weakly ferromagnetically coupled in the dimer.

Introduction

We have previously described the synthesis and some of the coordination properties of a new class of heteroscorpionate ligand (see below) of the general type L_2CX, where L = 3- and/or 5-substituted pyrazole and X = a functionalized donor, such as a substituted phenol or thiophenol.[1–4] We have shown that the nature of the metal complexes formed depends on the particular metal involved, the degree of substitution on the pyrazole arms, as well as the ligand to metal ratio. By varying the metal : ligand ratio it is possible to prepare not only the mononuclear ML_2 complexes, but also a series of homometallic di- and tri-nuclear species where, due to the basicity of the coordinated phenols, the octahedral complex functions as a ligand for another metal which is tetrahedrally coordinated.[4,5] We have recently extended some of this chemistry to include thiolate containing heteroscorpionates because of their biomimetic potential.[6]

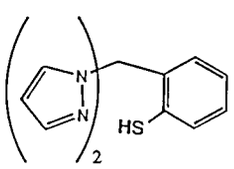

Mixed nitrogen–sulfur coordination of transition metals is a widely observed motif in biochemistry appearing in metalloproteins such as the "zinc-fingers", cupredoxins, isopenicillin *N*-synthase, nitrile hydratases and Reiske centers.[7] This type of coordination is also important in the biochemistry of nickel where several of the known types of nickel containing metalloproteins contain thiol or mixed N/O/S.[8–11] Thus, there has been considerable interest in the study of nickel thiolates and a large volume of interesting chemistry has been produced.[12–17] This body of work has, until recently, been concentrated on monomeric Ni thiolates. However, with the publication of the hydrogenase crystal structure, the focus now has shifted to homo- and hetero-bimetallic species.[18,19]

There have been a number of long standing problems in making tractable nickel thiolates. Primary among these is their strong tendency to oligomerize and polymerize in uncontrolled fashion to give ill characterized μ-thiolate bridged materials. Another is the pronounced preference for nickel(II) to adopt a square planar rather than tetrahedral geometry with these relatively strong field ligands. Also rare are bimetallic species with unsymmetrical mixed coordination numbers.[20] In this report we describe a number of Ni(II) complexes of the heteroscorpionate ligand (2-sulfanylphenyl)bis(pyrazolyl)methane, which while not intended to be accurate enzyme models, exhibit a number of interesting structural features which may make them useful platforms with which to prepare such in the future.

Experimental

All operations were carried out in air unless otherwise stated and the solvents used were of reagent grade or better (Aldrich Chemical Co.). MeCN was dried and degassed by distillation over CaH_2 under Ar(g). Diisopropyl ether was degassed and distilled over sodium–benzophenone under Ar(g). Microanalyses were performed by Desert Analytics Laboratory, Tucson, AZ. ^1H NMR spectra were obtained using a Varian INOVA 400 MHz FT-NMR system and all peaks are referenced to internal $SiMe_4$. IR spectra were recorded as KBr disks on a Perkin-Elmer 1600 series FT-IR. Solution electronic spectra were obtained using a Hewlett-Packard 8452A diode array spectrophotometer. Cyclic voltammetry and Osteryoung square wave voltammetry data were acquired using a Bioanalytical Systems CV-50W Voltammetric Analyzer System with a glassy carbon working and Pt secondary electrode, a BAS SCE reference, and 0.1 M $[^nBu_4N][PF_6]$ in nitromethane as

supporting electrolyte and solvent respectively. Resonance Raman spectra were acquired as previously described.[6] The synthesis of the ligand, (2-sulfanylphenyl)bis(pyrazolyl)methane hydrate, L5SH·H_2O, has been previously described.[6]

Synthesis

$[Ni_3(L5S)_4][ClO_4]_2·2H_2O·1.5Me_2CO$, 1. L5SH (0.20 g, 0.73 mmol) was dissolved in degassed acetone (12 ml) under an inert Ar(g) atmosphere. To this solution was added $Ni(ClO_4)_2·6H_2O$ (0.20 g, 0.55 mmol) which dissolved instantly causing a color change in the solution from very pale yellow to red. NaOMe (0.39 g, 0.73 mmol) was added to the reaction mixture causing an immediate intensification of the red color of the solution followed by the precipitation of a dark red solid. The reaction mixture was then stirred at RT for 30 min before the deep red solid was collected by filtration, washed with acetone (5 ml) and dried *in vacuo*. A portion of the product was redissolved in acetone and layered with $^iPr_2O$. Over a period of several days, very intense crimson block-like crystals of crystallographic quality were deposited. Yield: 0.17 g (67%) (Calc. for $C_{56.5}H_{57}N_{16}Cl_2Ni_3O_{11.5}S_4$: C, 44.65; H, 3.75; N, 14.75. Found: C, 44.91; H, 3.49; N, 14.67%). IR (cm^{-1}): 3123, 1405, 1289, 1100, 989, 863, 810, 752, 689, 626.

$[Ni_2(L5S)_2(MeCN)_4][BPh_4]_2·Me_2CO$, 2. L5SH (0.20g, 0.73 mmol), NaOMe (0.0394 g, 0.73 mmol), and $NaBPh_4$ (0.25 g, 0.73 mmol) were dissolved in acetone (10 ml) forming a pale yellow solution. $NiCl_2·6H_2O$ (0.17 g, 0.73 mmol) was added to the NaL5S–$NaBPh_4$ solution, quickly dissolving to form the deep crimson solution of the trimer. The reaction mixture was stirred for 30 min and then filtered to remove a small amount of precipitate. Pale green crystals of the dimer suitable for X-ray determination were produced by vapour diffusion of acetonitrile into the acetone supernatant at 4 °C. A small number of darker green crystals were also found in several of the samples and these were also subjected to X-ray analysis and proved to be $[Ni_2(L5S)_2(MeCN)_2(H_2O)_2]Cl_2·2.5H_2O$, the chloride salt of **3** (designated here as **3a**).

$[Ni_2(L5S)_2(MeCN)_2(H_2O)_2][ClO_4]_2·MeCN·H_2O$, 3. L5SH·$H_2O$ (0.20 g, 0.73 mmol) and $Ni(ClO_4)_2·6H_2O$ (0.32 g, 0.87 mmol) were dissolved in MeCN (10 ml) forming a pale yellow solution. Dropwise addition of triethylamine caused the dark red to fade very rapidly to an emerald green color. After the addition of 3 drops of triethylamine a pale green microcrystalline solid started to precipitate from the solution. After 5 drops, the solid was collected by filtration, washed with MeCN (5 ml), and dried *in vacuo*. Yield: 0.26 g (36%) (Calc. for $C_{32}H_{37}N_{11}Cl_2Ni_2O_{11}S_2$: C, 38.26; H, 3.69; N, 15.34; Cl, 7.07. Found: C, 38.36; H, 3.53; N, 15.09; Cl, 6.91%). IR (cm^{-1}): 3404, 3125, 2986, 1630, 1580, 1560, 1516, 1470, 1445, 1426, 1401, 1361, 1291, 1251, 1212, 1092, 992, 932, 873, 757, 683, 663, 628, 469.

$[Co_2(L5S)_2(MeCN)_4][BPh_4]_2·2MeCN$, 4. L5SH·$H_2O$ (0.20 g, 0.73 mmol), NaOMe (0.039 g, 0.73 mmol), and $NaBPh_4$ (0.19 g, 0.55 mmol) were dissolved in degassed, anhydrous MeCN (10 ml), under an Ar(g) atmosphere, forming a pale yellow solution. Separately, anhydrous $CoCl_2$ (0.095 g, 0.73 mmol) was dissolved in dry, degassed MeCN (5 ml), under Ar(g). The NaL5S–$NaBPh_4$ solution was transferred by cannula into the $CoCl_2$(MeCN) solution causing the instant precipitation of a brown solid. The solution was stirred at room temperature for 30 min before the mother-liquor was filtered into three small Schlenk tubes, each filled with Ar(g). The orange-brown solutions within each of these flasks were then carefully layered with anhydrous, degassed $^iPr_2O$ and were left to stand for a period of several days during which time brown block crystals formed on the sides of the tubes and the orange-brown solution had turned a deep green. The green color was due to oxidation of the Co(II) complex into the known monomeric Co(III) thiolate, $[Co(L5S)_2]^+$ by adventitious oxygen.[6] The brown crystals were used in the crystallographic determination.

X-Ray crystallography

Crystals of $[Co_2(L5S)_2(MeCN)_4][BPh_4]_2·2MeCN$, $[Ni_2(L5S)_2(MeCN)_4][BPh_4]_2·Me_2CO$, $[Ni_2(L5S)_2(MeCN)_2(H_2O)_2]Cl_2·2.5H_2O$, and $[Ni_3(L5S)_4][BPh_4]_2·xMe_2CO·x^iPr_2O$ of a quality suitable for crystallographic investigation were grown as described above. All crystals were sealed in thin-walled quartz capillaries to prevent loss of lattice solvent to which all these crystals were prone. The crystals were mounted on a Siemens P4 diffractometer with a sealed tube Mo-Kα X-ray source ($\lambda = 0.71073$ Å) and under computer control with installed Siemens XSCANS 2.1 software. Automatic searching, centering, indexing, and least-squares routines were carried out for each crystal with at least 25 reflections in the range, $20° \leq 2\theta \leq 25°$ used to determine the unit cell parameters. During the data collections, the intensities of three representative reflections were measured every 97 reflections, and any decay observed was empirically corrected for by the XSCANS 2.1 software during data processing. The data were also corrected for Lorentz and polarization effects and for $[Ni_2(L5S)_2(MeCN)_4][BPh_4]_2·Me_2CO$ for X-ray absorption, using a semi-empirical correction determined using ψ-scan data. Structure solutions for all these crystals were obtained *via* direct methods or by the Patterson function, and refinement on *F* using the SHELXTL-PC software package and for $[Co_2(L5S)_2(MeCN)_4][BPh_4]_2·2MeCN$ on F^2 using the SHELXS-93 package.[21] A summary of cell parameters, data collection conditions, and refinement results are presented in Table 1. Selected bond lengths and angles for **1**–**4** are found in Tables 2–5. Details pertinent to the individual refinements are outlined below.

Solution of the structure of **1** was effected by direct methods and the initial asymmetric unit appeared to contain one complete $[Ni_3(L5S)_4]^{2+}$ cation, and two $[BPh_4]^-$ anions. Isotropic refinement of these three groups additionally revealed the presence of several lattice solvent molecules. These included an ordered Me_2CO molecule at full occupancy, an ordered $^iPr_2O$ molecule at half occupancy, a disordered but recognizable $^iPr_2O$ molecule and one disordered Me_2CO with a major position at 0.65 occupancy and reasonably well defined but the minor(s) so disordered that no systematic pattern was discernible. Another two even more highly disordered solvent fragments were located on or about special positions, the molecular identity of which could not be ascertained and so these two groups of electron density peaks were refined isotropically solely as carbon atoms. All the non-hydrogen atoms were refined isotropically and upon convergence of this refinement the non-hydrogen atoms of the $[Ni_3(L5S)_4]^{2+}$ cation were refined anisotropically. Hydrogen atoms were included in calculated positions for the $[Ni_3(L5S)_4]^{2+}$ cation and the two $[BPh_4]^-$ anions using a riding model with fixed isotropic thermal parameters (no hydrogen atom positions were calculated for any of the lattice molecules or molecular fragments).

The crystal structure of **2** was solved by direct methods, the asymmetric unit of the initial solution containing one-half of a $[Ni_2(L5S)_2(MeCN)_4]^{2+}$ cation (the other half being generated by inversion) and a $[BPh_4]^-$ anion. Isotropic refinement of these two groups further revealed the presence of one lattice Me_2CO at half occupancy within the asymmetric unit. All non-hydrogen atoms were refined first isotropically and then anisotropically. Hydrogen atoms were then included in calculated positions in the final cycles of refinement using a riding model with fixed isotropic thermal parameters except for the solvent Me_2CO for which no hydrogen atoms were included.

Structural solution of **3a** by direct methods indicated the presence of one-half of a $[Ni_2(L5S)_2(MeCN)_2(H_2O)_2]^{2+}$ cation (containing a center of symmetry), and a Cl^- anion within

Table 1 Crystallographic data and data collection parameters for **1**, **2**, **3a** and **4**[a]

	$[Ni_3(L5S)_4][BPh_4]_2$	$[Ni_2(L5S)_2(MeCN)_4][BPH_4]_2$	$[Ni_2(L5S)_2(MeCN)(H_2O)_2]Cl_2$	$[Co_2(L5S)_2(MeCN)_4][BPh_4]_2$
Formula unit	$C_{117.6}H_{83}N_{16}B_2Ni_3O_{2.15}S_4$	$C_{44}H_{37}N_6B_1Ni_1O_1S_1$	$C_{15}H_{15}N_5Cl_1Ni_1O_{2.25}S_1$	$C_{43}H_{40}N_7B_1Co_1S_1$
Space group	$P2_1/c$	$C2/c$	$P2_1/n$	$C2/c$
a/Å	18.247(3)	19.940(2)	10.865(2)	20.299(2)
b/Å	30.143(4)	20.129(1)	9.582(1)	20.138(2)
c/Å	23.332(4)	19.671(2)		19.712(2)
β/°	109.07(1)	97.409(8)	100.21(1)	97.462(9)
V/Å^3	12128.3(40)	7829.8(12)	1801.70(61)	7989(2)
ρ/g cm^{-3}	1.139	1.258	1.564	1.258
Z	4	8	4	8
M	2080.6	767.1	424.1	755.8
Crystal size/mm	0.5 × 0.4 × 0.25	0.4 × 0.4 × 0.4	0.35 × 0.2 × 0.2	2 crystals[c]
Crystal color, habit	Crimson, block	Pale green, block	Emerald, block	Orange blocks
μ/mm^{-1}	0.582	0.588	1.329	0.521
2θ range/°	3.5–45.0	3.5–45.0	3.5–45.0	3.5–40.0
No. of unique data	11171	5065	2324	4005
No. of obs data	4986	2658	1082	3988[d]
Data: parameter ratio	5.0:1	5.4:1	4.7:1	8.23:1
Transmission factors		0.8110/0.9264		
R^b	8.42 [$I > 4\sigma(I)$]	5.30 [$I > 4\sigma(I)$]	6.27 [$I > 4\sigma(I)$]	7.28[e]
R_w[b]	10.07	5.94	6.58	17.15[e]
max diff peak, e Å^{-3}	+0.54	+0.31	−0.66	−0.531
Δ/σ(mean)	0.016	0.024	0.011	

[a] T = 298 K; radiation, Mo-Kα, scan type, θ–2θ. [b] Quantity minimized $\Sigma w(F_o - F_c)^2$. $R = \Sigma|F_o - F_c|/wF_o$. $R_w = [\Sigma w(F_o - F_c)^2/\Sigma(wF_o)^2]^{\frac{1}{2}}$. [c] Three partial data sets from two crystals were merged to give an adequate amount of data to solve and refine this crystal structure. Crystal sizes; 0.5 × 0.4 × 0.4 mm, and 0.7 × 0.7 × 0.6 mm. [d] This structure was solved and refined on F^2 using *all* data by use of the program SHELXS-93 for IBM-PC compatibles. [e] These are "equivalent" R and R_w residuals for data with [$I > 2\sigma(I)$].

Table 2 Significant bond lengths (Å) and angles (°) for $[Ni_3(L5S)_4][BPh_4]_2 \cdot x Me_2CO \cdot x {}^iPr_2O$

Ni1–S3	2.391(5)	Ni1–S4	2.395(6)
Ni1–N9	2.065(15)	Ni1–N11	2.085(17)
Ni1–N13	2.038(17)	Ni1–N15	2.071(17)
Ni2–S1	2.266(7)	Ni2–S2	2.276(5)
Ni2–S3	2.274(6)	Ni2–S4	2.264(5)
Ni3–S1	2.398(5)	Ni3–S2	2.422(7)
Ni3–N1	2.042(20)	Ni3–N3	2.083(16)
Ni3–N5	2.055(14)	Ni3–N7	2.087(14)
Ni1 · · · Ni2	3.398	Ni2 · · · Ni3	3.340
S3–Ni1–S4	83.6(2)	S3–Ni1–N9	90.5(4)
S4–Ni1–N9	171.1(5)	S3–Ni1–N11	93.1(4)
S4–Ni1–N11	87.8(4)	N9–Ni1–N11	85.9(5)
S3–Ni1–N13	169.4(5)	S4–Ni1–N13	89.3(5)
N9–Ni1–N13	97.4(6)	N11–Ni1–N13	94.6(6)
S3–Ni1–N15	87.8(4)	S4–Ni1–N15	91.8(4)
N9–Ni1–N15	94.6(6)	N11–Ni1–N15	178.9(6)
N13–Ni1–N15	84.4(6)		
S1–Ni2–S3	126.4(2)	S1–Ni2–S2	92.3(2)
S1–Ni2–S4	113.6(2)	S2–Ni2–S3	109.7(2)
S3–Ni2–S4	89.3(2)	S2–Ni2–S4	129.6(2)
S1–Ni3–N1	90.0(5)	S1–Ni3–S2	85.7(2)
S1–Ni3–N3	93.2(5)	S2–Ni3–N1	172.2(5)
N1–Ni3–N3	85.7(8)	S2–Ni3–N3	88.0(6)
S2–Ni3–N5	89.0(5)	S1–Ni3–N5	170.6(5)
N3–Ni3–N5	94.3(7)	N1–Ni3–N5	96.2(6)
S2–Ni3–N7	91.7(5)	S1–Ni3–N7	87.9(4)
N3–Ni3–N7	178.8(7)	N1–Ni3–N7	94.6(7)
N5–Ni3–N7	84.5(6)		
Ni1–S3–Ni2	93.5(2)	Ni2–S2–Ni3	90.6(2)
Ni1–S4–Ni2	93.6(2)	Ni2–S1–Ni3	91.4(2)

Table 3 Significant bond lengths (Å) and angles (°) for $[Ni_2(L5S)_2(MeCN)_4][BPh_4]_2 \cdot Me_2CO$

Ni1–S1	2.377(2)	Ni1–N1	2.064(6)
Ni1–N3	2.069(6)	Ni1–N5	2.100(7)
Ni1–N6	2.064(6)	Ni1–S1A	2.470(2)
Ni1 · · · Ni1A	3.500		
S1–Ni1–N1	96.1(2)	S1–Ni1–N3	88.5(2)
N1–Ni1–N3	87.0(2)	S1–Ni1–N5	173.8(2)
N1–Ni1–N5	89.3(2)	N3–Ni1–N5	88.8(3)
S1–Ni1–N6	87.5(2)	N1–Ni1–N6	176.3(3)
N3–Ni1–N6	94.1(3)	N5–Ni1–N6	87.2(3)
S1–Ni1–S1A	87.6(1)	N1–Ni1–S1A	88.7(2)
N3–Ni1–S1A	173.9(2)	N5–Ni1–S1A	95.6(2)
N6–Ni1–S1A	90.4(2)	Ni1–S1–Ni1A	92.4(1)

Table 4 Significant bond lengths (Å) and angles (°) for $[Ni_2(L5S)_2(MeCN)_2(H_2O)_2]Cl_2 \cdot 2H_2O$

Ni1–S1	2.393(4	Ni1–N1	2.040(12)
Ni1–N3	2.041(11)	Ni1–N5	2.048(13)
Ni1–O1	2.162(9)	Ni1–S1A	2.450(4)
Ni1 · · · Ni1A	3.512		
S1–Ni1–N1	95.4(4)	S1–Ni1–N3	87.3(3)
N1–Ni1–N3	88.8(5)	S1–Ni1–N5	90.9(4)
N1–Ni1–N5	173.6(5)	N3–Ni1–N5	91.0(5)
S1–Ni1–O1	175.6(3)	N1–Ni1–O1	87.9(4)
N3–Ni1–O1	89.9(4)	N5–Ni1–O1	85.8(4)
S1–Ni1–S1A	87.0(1)	N1–Ni1–S1A	90.0(3)
N3–Ni1–S1A	174.0(3)	N5–Ni1–S1A	90.9(4)
O1–Ni1–S1A	95.9(3)	Ni1–S1–Ni1A	93.0(1)

the asymmetric unit. Subsequent isotropic refinement also indicated the presence of two lattice water molecules, one at full occupancy and one at quarter occupancy. All non-hydrogen atoms were refined isotropically and then after convergence, anisotropically with the exception of the 0.25 occupancy water oxygen atom. Hydrogen atoms were included in calculated positions using a riding model with fixed isotropic thermal parameters except for the two lattice water molecules.

The crystals of **4** were extremely prone to degradation, either by loss of lattice solvent or by the X-ray beam. After several attempts to collect a complete data set from a single crystal set proved unsuccessful, a full data set was obtained by merging three partial data sets from two crystals. The structure was solved by direct methods with the asymmetric unit containing one-half $[Co_2(L5S)_2(MeCN)_4]^{2+}$ cation (related to its second half by a center of inversion), a $[BPh_4]^-$ anion, and a molecule of lattice MeCN solvent. All non-hydrogen atoms were refined isotropically and subsequently anisotropically. Upon convergence of the anisotropic refinement hydrogen atoms were included in calculated positions using a riding model with fixed isotropic thermal parameters except for the lattice MeCN

Table 5 Significant bond lengths (Å) and angles (°) for $[Co_2(L5S)_2(MeCN)_4][BPh_4]_2\cdot 2MeCN$

Co1–N6	2.102(12)	Co1–N1	2.103(12)
Co1–N5	2.113(11)	Co1–N3	2.117(10)
Co1–S1	2.398(3)	Co1–S1A	2.486(4)
Co1 · · · Co1A	3.433		
N6–Co1–N1	96.1(4)	N6–Co1–N5	85.9(4)
N1–Co1–N5	86.2(4)	N6–Co1–N3	176.0(4)
N1–Co1–N3	85.0(4)	N5–Co1–N3	90.3(4)
N6–Co1–S1	88.1(3)	N1–Co1–S1	88.1(3)
N5–Co1–S1	171.3(3)	N3–Co1–S1	95.8(3)
N6–Co1–S1A	89.7(3)	N1–Co1–S1A	174.0(3)
N5–Co1–S1A	95.6(3)	N3–Co1–S1A	89.3(3)
S1–Co1–S1A	90.72(12)	Co1–S1–Co1A	89.28(12)

molecule for which no hydrogen atoms were included in the structure factor calculation.

CCDC reference number 186/1313.

Results

Description of structures

The linear trimeric cation of **1**, $[Ni_3(L5S)_4]^{2+}$ (Fig. 1), contains three Ni^{2+} atoms in a linear arrangement similar to that seen with the phenolate analog.[4] The two terminal Ni^{2+} atoms are each coordinated to two $[L5S]^-$ ligands in a tridentate manner with the thiolate sulfur donor atoms arrayed in a *cis* geometry and bridging to a third Ni^{2+}, the central metal atom of the trimer. The S_4 ligated central Ni^{2+} has a slightly flattened tetrahedral geometry with a dihedral angle of 104° between the two $Ni_{terminal}S_2Ni_{central}$ planes. The S–Ni–S angles of this metal atom show some deviation from regularity, mainly due to the compression of the S1–Ni2–S2 and S3–Ni2–S4 angles to values of 92.3(2)° and 89.3(2)°, by formation of the $Ni_{terminal}S_2Ni_{central}$ 4-membered chelate ring which also causes a corresponding expansion of the S2–Ni2–S4 and S1–Ni2–S3 angles to values of 129.6(2)° and 126.4(2)°. The terminal 6-coordinate Ni^{2+} atoms have distorted octahedral geometries, the main source of the geometric distortion again being due to compression of the S2–Ni3–S1 and S3–Ni1–S4 angles by the formation of the $Ni_{terminal}S_2Ni_{central}$ chelate ring. The Ni–S bond distances of the central, psuedo-tetrahedral Ni^{2+} atom (average, 2.270 Å) are shorter than those of the distorted octahedral terminal Ni^{2+} atoms (average, 2.402 Å) due to their differing coordination numbers. The thiolate sulfur bridging ligands make angles averaging 92.28° with the three Ni^{2+} atoms of the linear trimeric $[Ni_3(L5S)_4]^{2+}$ cation mediating Ni–Ni separations of 3.398 Å (Ni1 · · · Ni2) and 3.340 Å (Ni2 · · · Ni3).

The structures of **2**, **3a** and **4** are all extremely similar and ORTEP views of **3a** and **4** are shown in Fig. 3 and 2 respectively. Each are dimers with two coordinatively unsaturated metals ions bound by one $L5S^-$ ligand apiece, the sulfurs of which bridge the two metals. The remaining two sites on each octahedrally coordinated metal ion are filled by solvent (MeCN and/or H_2O). There is a distinct asymmetry in the M–S bridging distances with the short bond averaging 2.389 Å and the long bond 2.469 Å suggesting that the dimers are relatively weakly associated in the solid state.

The bridging M–S–M and S–M–S angles all average nearly 90° giving rise to M–M separations near 3.481 Å (range 3.433–3.512 Å) which are slightly longer than those seen in the trimer. The M–N bonds show no obvious *trans* influence and the bond lengths for the pyrazole nitrogens and acetonitrile nitrogens are also similar. The Ni–O bond of **3a** at 2.162(9) Å is about 0.12 Å longer than the corresponding Ni–N bonds.

Synthesis and characterization

The linear trimer was first obtained in modest yield during the attempted synthesis of the $Ni(L5)_2$ complex using a 2:1 ligand to metal ratio. None of the expected monomeric product was ever isolated. Subsequently it was found that the trimer could be prepared in good yield using the requisite 4:3 ligand to metal ratio in acetone as a solvent.

The electrochemistry of **1** in nitromethane was dominated by an oxidative wave near +456 mV which is believed to represent the Ni(II)→Ni(III) oxidation, however, it is unclear if it is associ-

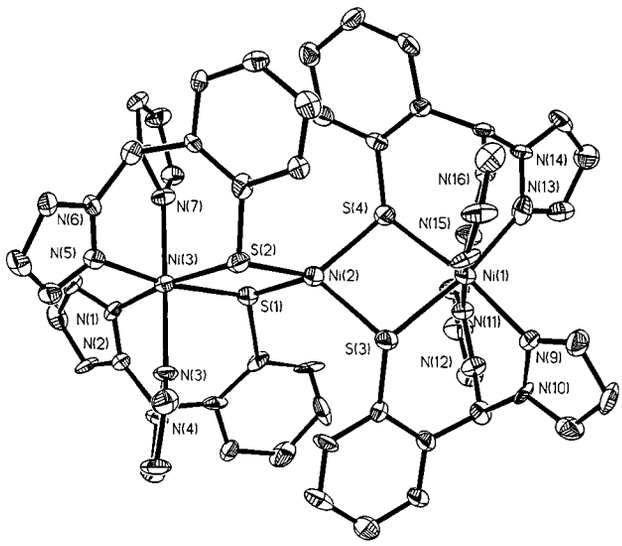

Fig. 1 Thermal ellipsoid view of the $[Ni_3(L5S)_4]^{2+}$ cation with selected atom labelling.

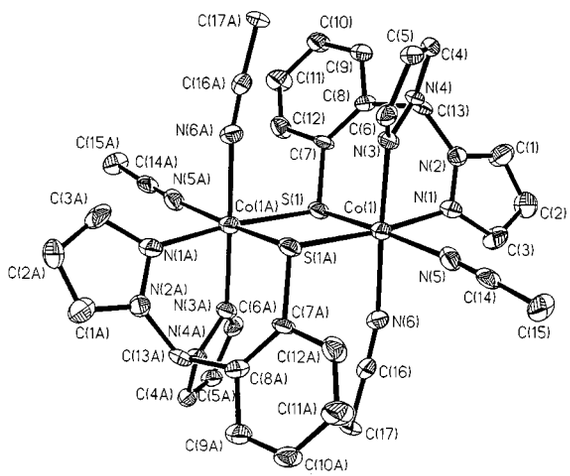

Fig. 2 Thermal ellipsoid view of the $[Co_2(L5S)_2(MeCN)_4]^{2+}$ cation with full atom labelling.

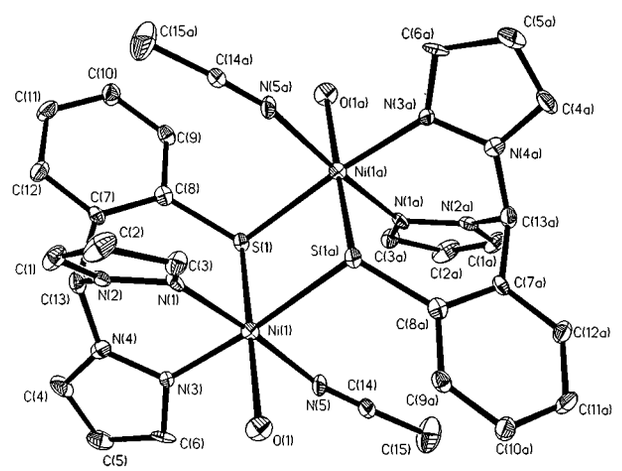

Fig. 3 Thermal ellipsoid view of the $[Ni_2(L5S)_2(MeCN)_2(H_2O)_2]^{2+}$ cation with full atom labelling.

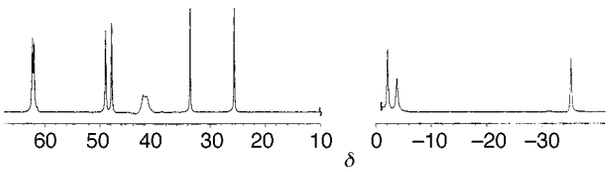

Fig. 4 Proton NMR spectrum of **1** in CD_3NO_2. The FID was processed with 10 Hz line broadening and a baseline correction applied. Solvent peaks in the diamagnetic region have been eliminated for clarity.

ated with the central, S4 coordinated, or the terminal, N4S2 coordinated, nickel. The data presented by Darensbourg *et al.* would suggest that the primary redox active site is the latter.[22]

The trimer **1** was only sparingly soluble in solvents in which it did not react being most soluble in acetone or nitromethane in which it formed intense red-violet solutions. Attempts to dissolve the trimer in acetonitrile, however, brought about a rapid color change from red to yellow and precipitation of a new complex which proved to be the dimer **2**. Indeed crystals of **2** were prepared by vapor diffusion of MeCN into acetone solutions of the trimer. Other alkyl- and aryl-nitriles gave similar results. Attempts to prepare bulk quantities of **2** showed that the coordinated acetonitriles were labile and exchanged with traces of water in the solvents thus producing **3**. The Co(II) analog of **2** could also be prepared but because of its extreme sensitivity to oxidation to the corresponding $Co(L5)_2^+$ it was not characterized further in solution.

NMR studies

While square planar complexes of Ni(II) are diamagnetic and hence amenable to NMR spectroscopy, octahedral and tetrahedral complexes are paramagnetic. Nevertheless due to relatively favorable electronic relaxation times, such paramagnetic species can also be examined by NMR spectroscopy, although under these conditions the peaks are strongly shifted from their diamagnetic positions and are broadened.[23] We have already reported the NMR spectra of mono-, di-, and trinuclear complexes of Ni(II) with the analogous phenolate containing heteroscorpionate ligands.[5] In contrast to the rather broad lines found in the latter, the trinuclear thiolate $[Ni_3(L5S)_4]^{2+}$ in d_3-nitromethane gives comparatively sharp resonances spread over approximately 100 ppm (Fig. 4). The 11 observed lines are consistent with the solution stability of the trinuclear dication and the presence of just a single isomer although we have not assigned the various resonances.

Dissolution of the sparingly soluble dinuclear $[Ni_2(L5S)_2(MeCN)_4]^{2+}$ cation in CD_3CN produces a spectrum with approximately seven weak and very broad lines seen over the range δ +70 to −30. Clearly, there are significant differences in the electronic relaxation times between the dimer and the trimer which render the dimer spectrum extremely broad and coupled with the compounds' low solubility, leave it barely observable.

As described earlier, the interconversions between the dinuclear and trinuclear species are solvent dependent and can be followed by NMR as well as optical spectroscopy. Thus, dissolving the dinuclear $[Ni_2(L5S)_2(MeCN)_4]^{2+}$ cation in nitromethane rather than MeCN produces a complex spectrum with one set of 11 sharp lines and another set of 11 or more very broad ones. The sharp lines correspond to those of $[Ni_3(L5S)_4]^{2+}$ in the same solvent, while the broad lines *do not* match those of the starting dimer in MeCN. The nature of the species responsible for the broad lines remains unknown at this time. Conversely, addition of CD_3CN to a CD_3NO_2 solution of the trinuclear cation causes the color to change from deep red to pale orange with a concomitant broadening and shifting of the peaks due to the trinuclear species into those of the dinuclear one. Increasing the concentration of CD_3CN in the solution causes a further color change to yellow and an NMR spectrum similar to that of the dimer in MeCN.

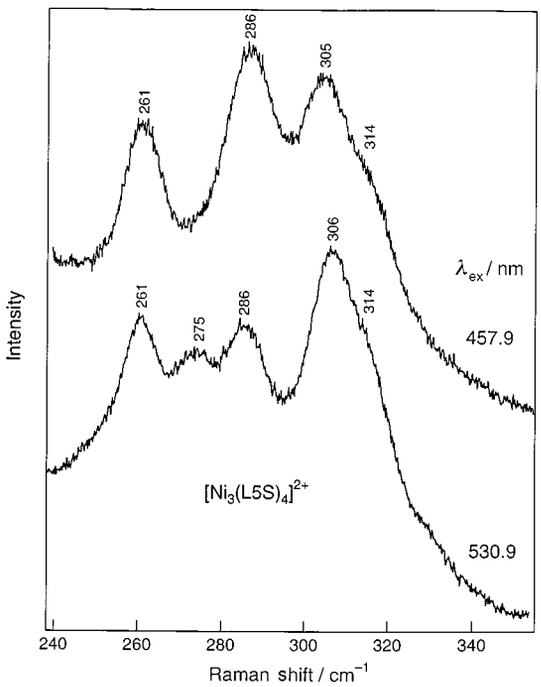

Fig. 5 Resonance Raman spectra of solid **1** with 457.9 and 530.9 nm excitation wavelengths, 150 mW laser power and 6 cm^{-1} slit width.

Optical and resonance Raman spectroscopy

The optical spectrum of **1** shows a strong band in the visible at 526 nm with a molar absorptivity (ε) of 5800 M^{-1} cm^{-1}. The magnitude of ε identifies this feature as a S→Ni charge transfer (CT) transition and hence amenable to resonance Raman (RR) analysis. The RR spectrum (Fig. 5) displays three strongly enhanced bands in the range 250–300 cm^{-1}. X-Ray crystallography of **1** shows the presence of two distinct Ni–S environments, one octahedral and one tetrahedral with bond distances varying from 2.26 Å to 2.40 Å. The Co–S bonding distances in the previously characterized $[Co(L5S)_2]^+$ are near 2.250 Å and the Co–S vibrational frequencies are observed at 312 and 333 cm^{-1}.[6] Since Co and Ni have similar atomic mass, the Ni–S vibrational frequencies should be close to those of Co–S if they both have similar bond distances. The tetrahedrally coordinated Ni2, has an average Ni–S bond distance of 2.270 Å. Therefore, the Ni–S frequencies of this Ni site should be near 300 cm^{-1}. The RR spectrum exhibits a strong band at 305 cm^{-1} with a shoulder at 314 cm^{-1}, in agreement with the predictions. However, there are also two other strong bands observed in the RR spectrum at 261 and 286 cm^{-1}. These two bands are believed to be Ni–S vibrational modes as well. Badger's rule predicts that the Ni–S vibrational frequency would down-shift from 305 cm^{-1} to 261 cm^{-1} with an increase in Ni–S bond distance from 2.270 Å to 2.420 Å.[24] Therefore, the enhanced bands at 261 and 286 cm^{-1} are from the octahedrally coordinated Ni(1) and Ni(3) which have the longer Ni–S bonds. The RR spectra also indicate a difference in the enhancement factors for these modes with varying excitation wavelengths. Under violet-blue excitation, the bands at 261 and 286 cm^{-1} are more enhanced than the band around 300 cm^{-1}, while the band around 300 cm^{-1} is more enhanced under the yellow excitation. This correlates with the major visible absorption band and implies that the S→Ni CT band at 526 nm is derived from the central tetrahedral Ni. The S→Ni CT transitions from the octahedral nickels are found at higher energy consistent with the maximal enhancement with violet-blue excitation. The optical spectrum of **3** which contains only octahedrally coordinated Ni has no strong bands in the visible region of the spectrum with only a weak d–d band observed at 568 nm (ε = 77 M^{-1} cm^{-1}). A strong shoulder in the near-UV at 388 nm

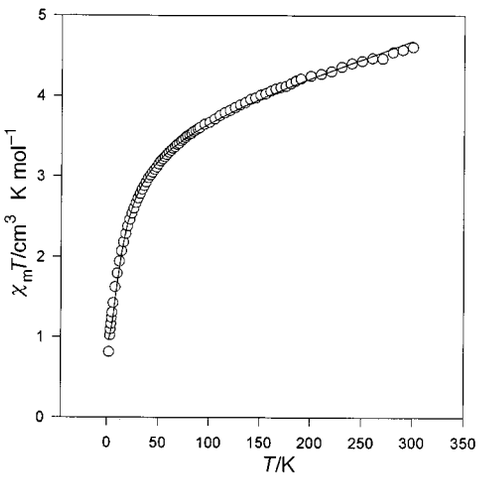

Fig. 6 Plot of $\chi_m T$ *vs.* T for **1**. The open circles represent the data, the solid line the theoretical fit to the single J model described in the text.

($\varepsilon = 2180$ M^{-1} cm^{-1}) does, however, appear which we assign as the octahedral S→Ni CT consistent with the RR results on **1**.

Magnetics

We have obtained variable temperature magnetic data on compounds **1** and **3** and completed a preliminary analysis (Fig. 6). For the Ni trimer, **1**, $\chi_m T$ decreases from about 4.5 at 300 K to 0.9 cm^3 K mol^{-1} at 2 K suggesting an $S = 1$ ground state with some significant population of higher moment states of a spin ladder. The trimer data has been fitted to the HDVV (Heisenberg–Dirac–Van Vleck) spin Hamiltonian for linear trinuclear complexes [eqn. (1)] where $S_1 = S_2 = S_3 = 1$ and $J_{12} = J_{23}$.

$$\begin{array}{c} \mathrm{A}\cdots\mathrm{A}\cdots\mathrm{A} \\ S_1\ S_2\ S_3 \end{array}$$

$$H_{\mathrm{exch}} = -2[J_{12}\cdot S_1\cdot S_2 + J_{23}\cdot S_2\cdot S_3 + J_{13}\cdot S_1\cdot S_3] \quad (1)$$

The theoretical expression for $\chi_m T$ can be found in ref. 25. To minimize the number of independent parameters we have assumed that the g values for both the terminal and central Ni atoms are identical. Good fits to the data could be obtained using both a terminal and adjacent coupling constant where $J_{12} = +9.80$ cm^{-1}, $J_{13} = -14.34$ cm^{-1}, $g = 2.07$, and temperature independent paramagnetism (TIP) of 0.0047. However, a slightly better fit, derived from a model which assumed that the terminal coupling was vanishingly small and a molecular field correction, was applied to account for weak *intermolecular* interactions.[26] This leads to $g = 2.17$, $J = -2.69$ cm^{-1}, $z'J' = -0.33$ cm^{-1} and TIP = 0.0042. In either case the overall interaction between the nickels is weakly antiferromagnetic.

For the Ni dimer, **3**, $\chi_m T$ is seen to rise slowly from about 3.3 cm^3 K mol^{-1} at 300 K reaching a peak of 3.7 cm^3 K mol^{-1} at 25 K before falling away rapidly at lower temperature. This behavior is indicative of overall weak intradimer ferromagnetic coupling with either or both zero field splitting (ZFS) and intermolecular antiferromagnetic interactions accounting for the decrease in $\chi_m T$ at very low temperature. The data was fitted to a model derived by Ginsberg which includes terms for the intradimer coupling (J), the ZFS parameter (D), and the molecular field correction ($z'J'$).[27] Best fits, which were only fair however, gave $D = +2.0$ cm^{-1}, $J = +5.5$ cm^{-1}, $g = 1.8$ and $z'J' = -0.31$ cm^{-1}.

Discussion

The concept of metal complexes which themselves function as ligands for other metals is well known. In particular, metal complexes containing *cis* oriented phenolates or thiolates possess sufficient electron density at these atoms to function as donors and bridge to exogenous metals.[4,28] Thus thiolate bridged trimers of Ni(II) with N,S chelates are in themselves quite common, however, virtually all of these complexes have the central Ni(II) in a square planar S_4 geometry.[22,29–31] This is the expected result since with relatively strong field donors such as thiolates the d^8 configuration strongly prefers such a geometry. Thus, the near tetrahedral geometry adopted by the central Ni in **1** is unusual. In fact, non-macromolecular Ni(II) complexes with S_4 pseudo-tetrahedral geometry are rare, the $[Ni(SR)_4]^{2-}$ (R = aryl) anions being the only examples of which we are aware.[32] Clearly in the case of **1** steric clashes between the thiophenolate rings of the $Ni(L5S)_2$ units prevent square planar coordination. However, there must be electronic factors as well since the phenolate analog which has shorter Ni–X bonds and would therefore be expected to be more sterically congested than **1** adopts a less tetrahedral like geometry (dihedral angle of 64° *vs.* 86° in **1**).[4] The structural parameters for the central Ni in **1** *i.e.* Ni–S bond lengths and angles about the Ni–S4 "tetrahedron" are quite similar to those reported for the $[R'_4N]_2[Ni(SR)_4]$ complexes.[32]

Resonance Raman spectroscopy shows that the major band in the visible region of the optical spectrum of **1** is a S→Ni CT terminating at the central tetrahedrally coordinated nickel. Both Ni(II) substituted rubredoxin and the $[Ni(SR)_4]^{2-}$ anion have strong LMCT bands in the 300–500 nm range.[32,33] The red shift seen for the LMCT in **1** is due to the fact that it is a dication rather than a dianion which is expected to make the formal photoreduction of the Ni(II) center occur at lower energy.

The solution behavior of **1** is indicative of equilibria such as those described below:

$$[L_2NiNiNiL_2]^{2+} + 2MeCN \longrightarrow [L_2NiNi(MeCN)_2]^{2+} + NiL_2 \quad (2)$$

$$[L_2NiNi(MeCN)_2]^{2+} + 2MeCN \longrightarrow [LNi(MeCN)_2NiL(MeCN)_2]^{2+} \quad (3)$$

We depict this reaction as going through a $[L_2NiNi(MeCN)_2]^{2+}$ intermediate with mononuclear NiL_2 as the other product, neither of which have been isolated . However, there is precedence for this type of chemistry occurring with the phenolate analog[5] of **1** *i.e.*

$$[L_2MMML_2]^{2+} + 2X^- \longrightarrow [L_2MM(X)_2] + ML_2 \quad (4)$$

$$[L_2MM(X)_2] + 2X^- \longrightarrow ML_2 + MX_4^{2-} \quad (5)$$

In the absence of a good donor solvent the dinuclear product **2** can be desolvated whereupon it returns to the linear trimer as evidenced by NMR and optical spectroscopy.

$$2[LNi(MeCN)_2NiL(MeCN)_2]^{2+} + \text{excess } CH_3NO_2 \longrightarrow [L_2NiNiNiL_2]^{2+} + Ni(MeCN)_4^{2+} \quad (6)$$

The magnetic data for the Ni thiolate complex, **1**, can be compared to the trinuclear complexes prepared by ourselves,[4] Wieghardt[28] and Ginsberg.[34] In the case of the face sharing all octahedral systems reported by the latter two authors with acac or phenolate bridges, the overall ground state is $S = 3$ with a dominant ferromagnetic adjacent coupling (*ca.* +12–15 cm^{-1}) and a smaller antiferromagnetic (−4 to −6 cm^{-1}) terminal interaction.[28] The ferromagnetic ground state is attributed to the orthogonality of the magnetic orbitals due to the near 90° bridging angle. In the case of the thiolate bridged analog, the relative sign of the coupling has been reversed with $J_{12} = -28$ cm^{-1} and $J_{13} = +12$ cm^{-1}, the resulting ground state being $S = 1$.[28] The rationalization for this result is that the more acute bridging angle (*ca.* 75°) removes the accidental orthogonality

between the magnetic orbitals and that a new antiferromagnetic superexchange pathway becomes available due to the better energy match between the metal 3d orbital and the sulfur 3s orbitals. In the case of the thiolate bridged **3**, the magnetic orbitals are the t_2 on the tetrahedral Ni and the e_g on the octahedral. As pointed out by Wieghardt *et al.* it is possible with a near 90° bridging angle to orient these orbitals to give net overlap with a filled p orbital on the bridging sulfur of the type $e_g \| p \| t_2$.[35] This interaction would give rise to an antiferromagnetic superexchange pathway and indeed the overall interaction in **1** is antiferromagnetic with an $S = 1$ ground state. In the case of **3** the net ferromagnetism can be rationalized *via* the Goodenough–Kanamori rules from the presence of orthogonal overlaps of the type $e_g \| p_x \perp p_y \| e_g$ brought about by the near 90° bridging angles. However, in this case the situation can be complicated by a need to include the *intraionic* spin coupling term (D) that is often of the same order of magnitude as the *interionic* J coupling and powder data is rather insensitive to the combined variance of D and $z'J'$.[26] Thus, the fitted values should be viewed with caution. Nevertheless the values obtained for **3** are quite similar both in magnitude and sign to those obtained by Ginsberg[34] for a series of dibridged Ni dimers where D varied from +6.5 to +4.7 cm^{-1}, J from +9.7 to +4.9 cm^{-1} and $z'J'$ from −0.2 to −0.4 cm^{-1}.

Acknowledgements

This work was supported by Grants AI-1157 (to C. J. C.) and E-1184 (to R. S. C.) from the Robert A. Welch Foundation and NSF CHE-9726488 (C. J. C). The NSF-ILI program grant USE-9151286 is acknowledged for partial support of the X-ray diffraction facilities at Southwest Texas State University. C. J. O wishes to acknowledge partial support of this work by DARPA grant MDA972-97-1-0033.

References

1 T. C. Higgs and C. J. Carrano, *Inorg. Chem.*, 1997, **36**, 291.
2 T. C. Higgs and C. J. Carrano, *Inorg. Chem.*, 1997, **36**, 298.
3 T. C. Higgs R. S. Czernuscewicz and C. J. Carrano, *Inorg. Chim. Acta*, 1998, **14**, 273.
4 T. C. Higgs, K. Spartalian, C. J. O'Connor, B. F. Matzanke and C. J. Carrano, *Inorg. Chem.*, 1998, **37**, 2263.
5 T. C. Higgs, N. S. Dean and C. J. Carrano, *Inorg. Chem.*, 1998, **37**, 1473.
6 T. C. Higgs, D. Ji, R. S. Czernuscewicz, B. F. Matzanke, V. Schunemann, A. X. Trautwein, M. Helliwell, W. Ramirez and C. J. Carrano, *Inorg. Chem.*, 1998, **37**, 2383.
7 R. H. Holm, P. Kennepohl and E. I. Solomon, *Chem. Rev.*, 1996, **96**, 2239.
8 J. Xia, Z. Hu, C. V. Popescu, P. A. Lindahl and E. Munck, *J. Am. Chem. Soc.*, 1997, **119**, 8301.
9 A. Volbeda, M. H. Charon, C. Piras, E. C. Hatchikian, M. Frey and J. C. Fontecilla-Camps, *Nature* (*London*), 1995, **373**, 580.
10 A. L. de Lacey, E. C. Hatchikian, A. Volbeda, M. Frey, J. C. Fontecilla-Camps and V. M. Fernandez, *J. Am. Chem. Soc.*, 1997, **119**, 7181.
11 Z. Gu, J. Dong, C. B. Allan, S. B. Choudhury, R. Franco, J. G. Moura, I. Moura, J. Legall, A. E. Przybyla, W. Roseboom, S. P. J. Albracht, M. J. Axley, R. A. Scott and M. J. Maroney, *J. Am. Chem. Soc.*, 1996, **118**, 11155.
12 M. Kumar, R. O. Day, G. J. Colpas and M. J. Maroney, *J. Am. Chem. Soc.*, 1989, **111**, 5974.
13 H. J. Kruger, G. Peng and R. H. Holm, *Inorg. Chem.*, 1991, **30**, 734.
14 M. Cha, C. L. Gatlin, S. C. Critchlow and J. A. Kovacs, *Inorg. Chem.*, 1993, **32**, 5868.
15 S. C. Shoner, M. M. Olmstead and J. A. Kovacs, *Inorg. Chem.*, 1994, **33**, 7.
16 N. Baidya, M. M. Olmstead and P. K. Mascharak, *J. Am. Chem. Soc.*, 1992, **114**, 9666.
17 D. K. Mills, Y. M. Hsiao, P. J. Farmer, E. V. Atnip, J. H. Reibenspies and M. Y. Darensbourg, *J. Am. Chem. Soc.*, 1991, **113**, 1421.
18 C. Lai, J. H. Reibenspies and M. Y. Darensbourg, *Angew. Chem., Int. Ed. Engl.*, 1996, **35**, 2390.
19 F. Osterloh, W. Saak, D. Haase and S. J. Pohl, *Chem. Commum.*, 1997, 979.
20 S. Brooker and P. D. Croucher, *Chem. Commun.*, 1997, 459.
21 G. M. Sheldrick, SHELXTL-PC, Version 4.1, Siemens X-ray Analytical Instruments, Inc., Madison, WI, 1989.
22 P. J. Farmer, J. H. Reibenspies, P. A. Lindahl and M. Y. Darensbourg, *J. Am. Chem. Soc.*, 1993, **115**, 4665.
23 G. N. La Mar and W. Horrocks, (Editors), *NMR of Parmagnetic Molecules; Principles and Applications*, Academic Press, New York, 1973.
24 R. M. Badger, *J. Chem. Phys.*, 1934, **2**, 128.
25 O. Kahn, *Molecular Magnetism*, VCH Publishers, Weinheim, 1993.
26 C. J. O'Connor, *Prog. Inorg. Chem.*, 1982, **29**, 203.
27 A. P. Ginsberg, R. W. Martin, R. L. Brookes and R. C. Sherwood, *Inorg. Chem.*, 1972, **11**, 2884.
28 T. Beissel, F. Birkelbach, E. Bill, T. Glaser, F. Kesting, C. Krebs, T. Weyhermuller, K. Wieghardt, C. Butzlaff and A. X. Trautwein, *J. Am. Chem. Soc.*, 1996, **118**, 12376.
29 M. A. Turner, W. L. Driessen and J. Reedijk, *Inorg. Chem.*, 1990, **29**, 3331.
30 W. Tremel, M. Kriege, B. Krebs and G. Henkel, *Inorg. Chem.*, 1988, **27**, 3886.
31 M. G. B. Drew, D. A. Rice and K. M. Richards, *J. Chem. Soc., Dalton Trans.*, 1980, 2075.
32 S. G. Rosenfield, W. H. Armstrong and P. K. Mascharak, *Inorg. Chem.*, 1986, **25**, 3014.
33 A. T. Kowal, I. C. Zambrano, J. J. Moura, I. Moura, J. LeGall and M. K. Johnson, *Inorg. Chem.*, 1988, **27**, 1162.
34 A. P. Ginsberg, R. L. Martin and R. C. Sherwood, *Inorg. Chem.*, 1968, **7**, 932.
35 T. Beissel, T. Glaser, F. Kesting, K. Wieghardt and B. Nuber, *Inorg. Chem.* 1996, **35**, 3936.

Paper 8/08164F